Extreme Weather and PV Performance

Dirk C. Jordan, *Member, IEEE*, Kirsten Perry, *Member, IEEE*, Robert White, and Chris Deline, *Senior Member, IEEE*

***Abstract*—The impact of extreme weather events on photovoltaic (PV) performance was studied by comparing the National Oceanic and Atmospheric Administration database on severe weather with the National Renewable Energy Laboratory's PV Fleet database on continuous PV performance. We identified 170 systems that were immediately impacted by weather events. These severe weather events lead to a median loss of only 1% of annual production. However, flooding and high wind events were found to have an extremely long tail extending to 60% loss, showing that these discrete events can pose a substantial risk to PV systems. Besides the short-term impact of lost production due to outages, we also found a statistically significant increased performance loss rate (PLR) for high wind events above 90 km/h, by comparing PLR before and after these events. Similarly, hail events caused higher PLR for hail sizes of and above 25 mm indicating that more stringent hail testing for PV modules is required. In addition, very high snow loads may also cause increased PLRs, but more data are required to better quantify the impact. These findings illustrate the substantial risk extreme weather events pose short- and long-term to fielded PV installations.**

***Index Terms*—Degradation, durability, extreme weather, performance, photovoltaics (PVs), reliability.**

I. Introduction

EXTREME weather events have been increasing in frequency and intensity and are expected to further increase as global temperature increases. Fig. 1 shows an itemization of weather disasters in the USA, each exceeding the cost of inflation-adjusted one billion U.S. dollars [1]. This dataset goes back only to 1980, but an increase in the frequency of these major weather disasters is apparent, especially for severe storms. In the last 7 years alone, the accumulated cost of these events exceeds the almost unimaginable sum of one trillion U.S. dollars. And this is only for the USA; global numbers will be much greater and regularly make headline news. On the one hand, these types of events are expected to increase with climate change; and on the other hand, photovoltaic (PV) is one of the major technologies that could help to limit global temperature rises [2].

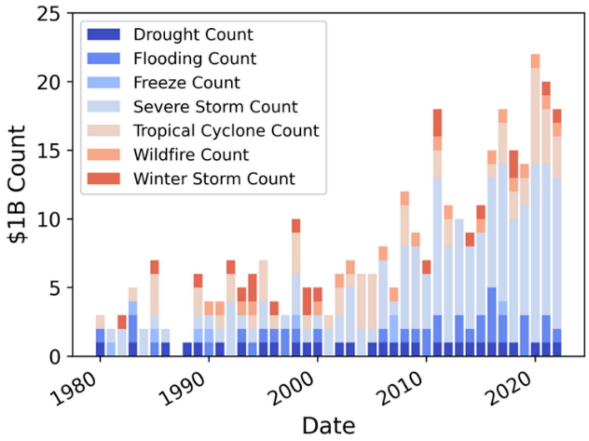

Fig. 1. Historical development of extreme weather events in the USA, each exceeding inflation-adjusted one billion U.S. dollars.

The natural following question is how do these weather events impact already deployed PV?

To address this question, we cross-compared one of the largest databases on extreme weather events in the world by the National Oceanic and Atmospheric Administration (NOAA) with one of the largest databases on time-series-based PV from the PV Fleet Performance Data initiative [3]. The associated PV Fleet database contains more than 24 000 inverter data streams from almost 2500 commercial and utility PV sites, totaling more than 8 Gigawatts, with a mean site age of more than 5 years [4].

Although this article is limited to events and deployments in the USA, we hope to inspire similar studies on other continents, and to possibly identify opportunities for future efforts on infrastructure hardening.

II. Methodology

The Storm Events Database, available publicly from NOAA, was queried, with the intent of comparing specific storm information to PV system data [5]. Specifically, events ranging from 2008 to present were collected. The Storm Events dataset is a compilation of reported storm occurrences and unusual weather phenomena occurring across the USA, and includes information on the event type (floods, hail, wind, tornadoes, etc.), start and end dates of the event, and beginning and end latitude–longitude coordinates associated with the event. To cross-compare with this weather dataset, PV system production data from the PV Fleets database was used. In total, this database contains over 56 billion records of PV time series data, including metadata,

Manuscript received 2 June 2023; revised 18 July 2023; accepted 4 August 2023. Date of publication 21 August 2023; date of current version 7 November 2023. This work was supported in part by the Alliance for Sustainable Energy, LLC, the manager and operator of the National Renewable Energy Laboratory for the U.S. Department of Energy under Grant DE-AC36-08GO28308; and in part by the U.S. Department of Energy's Office of Energy Efficiency and Renewable Energy under Solar Energy Technologies Office under Grant 30295. *(Corresponding author: Dirk C. Jordan.)*

The authors are with the National Renewable Energy Laboratory, Golden, CO 80401 USA (e-mail: dirk.jordan@nrel.gov; kirsten.perry@nrel.gov; robert.white@nrel.gov; chris.deline@nrel.gov).

Color versions of one or more figures in this article are available at https://doi.org/10.1109/JPHOTOV.2023.3304357.

Digital Object Identifier 10.1109/JPHOTOV.2023.3304357

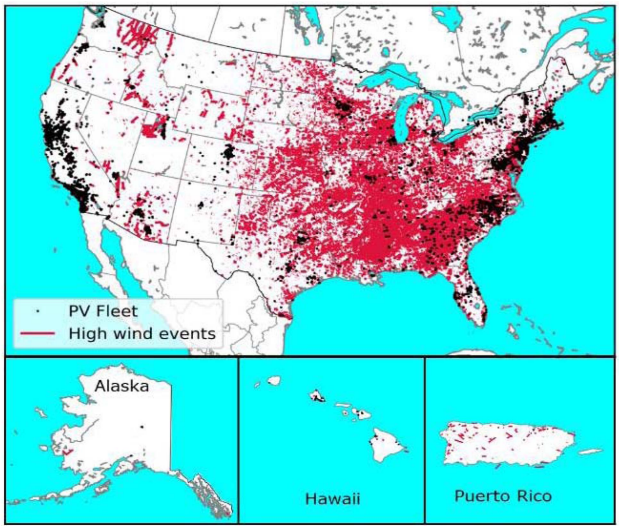

Fig. 2. Map of extreme weather events (high wind events) in red and overlaid the systems in the PV fleet database.

such as latitude–longitude coordinates, system capacity, azimuth, and tilt, as well as measured PV system performance data.

As an example, Fig. 2 shows a map of high wind events for the USA and Puerto Rico overlaid by PV Fleet systems. To build relationships between storm data and PV system data, the latitude–longitude coordinates associated with each storm event were compared to PV system latitude–longitude coordinates. Specifically, storm events within 10 km of a PV system, occurring during a period where measured time series data for that system were available, were marked for further analysis. After building this subset of storm events, associated system power data were plotted for each storm event. Each event was scrutinized for changes in power time series behavior within one calendar day of the event occurring. Cases where storm events coincided with flatlines or outages in system power data were compiled for a final resulting dataset. Overall, this dataset consists of 199 storm events associated with 170 distinct crystalline silicon systems. It is important to note that multiple storm effects can be associated with a single storm. For example, flooding and heavy rain could occur within hours over a single storm, and both events would be considered contributors to a PV system outage. Additionally, individual systems can be associated with multiple storm-related outages. Fig. 3 provides a breakdown of storm periods by event type. Most storms were predominantly associated with flooding and rain, followed by high winds.

Following the dataset compilation, additional variables associated with each outage were determined, including, classifying if the outage was full (all power streams affected) or partial (not all power streams affected) and calculating the length of the system outage in hours. For high wind events, we consolidated subcategories of thunderstorm and marine wind events including hurricanes, funnel clouds, tornadoes, dust devils, and waterspouts. An example of a high wind event in April of 2020 causing a partial outage is shown in Fig. 4.

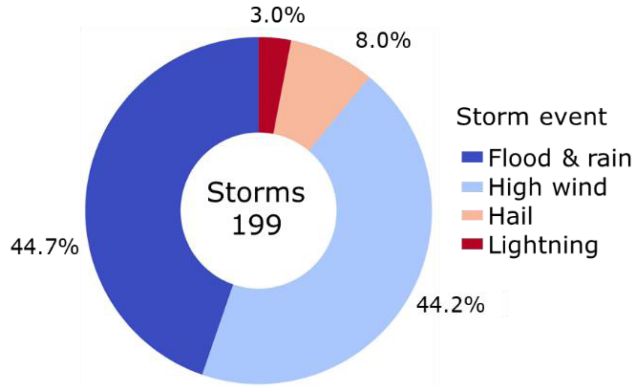

Fig. 3. Itemization of the type of storms that were within 10 km of a PV fleet system.

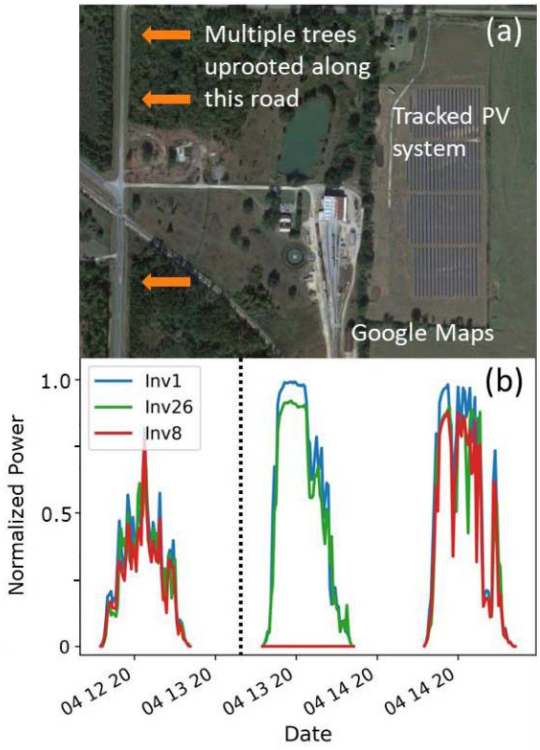

Fig. 4. Example of a PV system impacted by a high wind event. Multiple trees were uprooted along the road adjacent to the PV system (a). Time series of normalized power shows a partial outage for 1 of the 26 inverters the day following the extreme wind event (b), which is indicated by a vertical dashed line.

III. Short-Term Impacts

Full and partial outages immediately impact the power production following the weather event and are summarized in Fig. 5 as a cumulative distribution function (CDF) of the annual lost production in percent. The number of data points contained in the CDF are given by the number of systems with lost production and are provided along with other details in Table I. Here, lost power is tabulated as difference between actual production and expected (modeled) production, expressed as a percentage of annual generation.

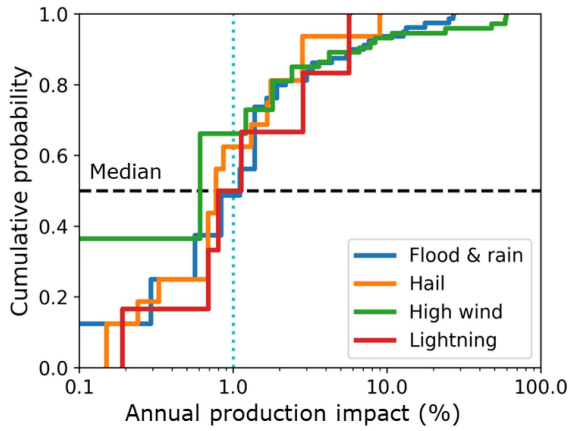

Fig. 5. Cumulative distribution function of the annual production impact caused by the extreme weather event. The median is indicated by a horizontal dashed line. A 1% impact is marked by a dotted cyan vertical line.

TABLE I
SUMMARY OF WEATHER EVENTS

Event type	Total systems	Systems impacted (%)	Systems with lost production	Lost production median (%)	Lost production mean (%)
Flood and rain	2716	2.7	74	1.1	2.6
Hail	1010	1.6	16	0.8	1.6
High wind	2293	3.2	74	0.7	4.0
Lightning	437	1.4	6	1.0	1.9

The impact of hail and high wind events are slightly below 1%, which appears reassuring. However, it should also be noted that flooding and high wind events have a long tail stretching to 60% of lost production. Therefore, despite statistically moderate losses of ca. 1% at the median, individual heavily impacted systems can experience a tremendous impact from extreme weather. This could reflect the difference between a system being peripherally impacted by a storm (e.g., temporarily losing grid connectivity) or the much less likely case of being physically damaged by it.

Of course, installation quality, supervision, and maintenance practices also can influence the impact of extreme weather, but this requires more detailed investigation of maintenance tickets, presenting a great follow-up study.

IV. Long-Term Impact

Beyond the immediate impacts of discrete weather events, long-term impacts in the form of performance loss rate (PLR) could be affecting systems for many years following an extreme weather event. Hail impacts or mechanical loads—dynamic or static—from wind or snow can lead to cell cracking within modules, the performance loss effect of which on power loss is still an active research area [6], [7]. In this article, we use

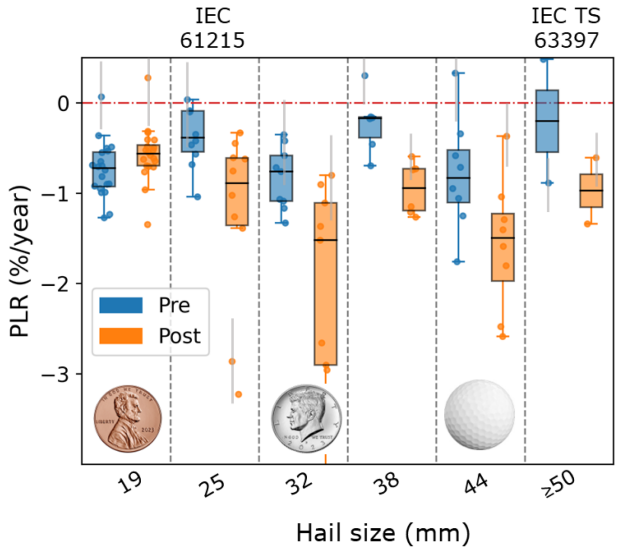

Fig. 6. RdTools analysis of performance loss rates pre-(blue) and poststorm (orange) for hail events on all systems, even if no outage was detected, immediately following the event. The extent of the boxplot represents the interquartile range with the median displayed by a horizontal line within each box. A representative uncertainty bar for each category is indicated by a gray vertical bar. For size comparison, a USA penny, half-dollar coin, and a golf ball are shown. The module qualification standard IEC 61215 and technical specification IEC 63397 are shown in their respective hail testing category.

RdTools, a freeware codeveloped by National Renewable Energy Laboratory using the year-on-year methodology to calculate PLRs [8]. Because the year-on-year method requires at least 2 years of data, we investigated all impacted systems that had at least 2 years of data prior and following a weather event. For irradiance data, we used satellite data from the National Solar Radiation Database (NSRDB) to avoid potential confounding effects because of irradiance sensor drift [9]. To reduce noise in the RdTools analysis, we further filtered for clear sky conditions [10]. Additionally, a 7-day moving Hampel outlier filter was used to remove outliers from the time series. These added steps allowed us to detect smaller changes in PLR when systems were exposed to hail wind or extreme snow events.

A summary of PLRs on systems impacted by hail of various sizes regardless of outage detection following the storm is presented in Fig. 6. Boxplots of the distributions in each category are shown using blue for PLRs before the storm (pre) and orange after the storm (post). Individual data points are overlaid on the boxplots with a representative uncertainty bar displayed by gray vertical bars that is calculated as the median from all uncertainty bars in each category. The no performance loss line is indicated by a horizontal red dash-dotted line. Additional information on the number of systems, inverters, and distribution parameters in each category are provided in Table II.

Despite PLR uncertainties and without exception, larger hail categories exhibited higher PLRs after hail impact, possibly indicating that initial impact needs to be combined with thermal cycling that actual installations experience, as published in IEC technical specification (TS) 63397. In summary, it appears possible that larger hail sizes may not necessarily lead to higher PLRs, rather it appears that higher PLRs will occur

TABLE II
SUMMARY OF HAIL-IMPACTED SYSTEMS

Hail size (mm)	Time	Inverters	Systems	Median PLR (%/year)	Interquartile range (%/year)
19	pre	20	3	−0.72	0.40
19	post	20	3	−0.56	0.27
25	pre	10	5	−0.38	0.54
25	post	10	5	−0.89	1.19
32	pre	9	3	−0.76	0.62
32	post	9	3	−1.52	1.92
38	pre	6	3	−0.17	0.47
38	post	6	3	−0.94	0.53
44	pre	8	4	−0.83	0.80
44	post	8	4	−1.49	1.20
≥50	pre	2	2	−0.20	1.37
≥50	post	2	2	−0.97	0.73

if a minimum damage threshold is exceeded. These findings should be corroborated with more detailed data and actual hail measurements because often the reported hail size is made by individual spotters and may not be as accurate as actual hail measurements.

Each hail category exhibits a statistically significant higher PLR after the storm except the first category (19 mm hail), the size of a U.S. penny coin. In the 19 mm category, the median PLR after hail shows slightly less loss than before hail. The difference is within the uncertainty and is most likely caused by measurement inaccuracies or subtle data quality issues that can be exacerbated for short monitoring periods. However, it is also conceivable that modules were replaced after the hail event. The module qualification test IEC 61215 uses 25 mm diameter sized hail [11]. Yet, systems exposed to 25 mm hail in the field displayed higher PLR despite being qualified to this specific hail size. Several possibilities exist that could explain the discrepancy. In naturally occurring hailstorms, many strikes may impinge on a module below the maximum determined hail size, yet potentially deliver more kinetic energy to a module [12]. In addition, actual hail is often not perfectly round and may not resemble indoor testing. Differences in mounting may also exist between indoor testing and actual field installation. Regardless of the underlying cause, the need for more stringent hail testing is evident from these data and is currently under development and published as TS IEC TS 63397 in 2022 [13].

Fig. 7 displays a similar graph for high wind events. Here pre and postevent PLR comparisons are split into four categories by maximum observed windspeed of the event. As with hail-impacted systems, it appears that a minimum windspeed threshold is required for accelerated degradation to occur after storm events. Similar to the hail analysis, the lowest wind category shows a median PLR after the windstorm with slightly less loss than before. In the same way, this difference can most likely be attributed to measurement uncertainty, although module replacement cannot be excluded from the time series

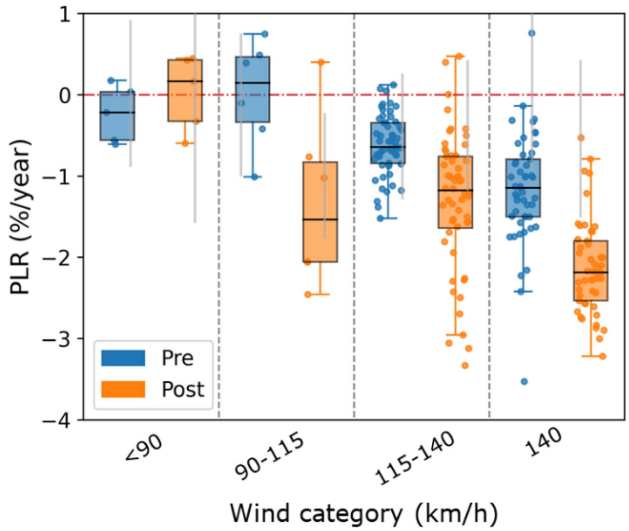

Fig. 7. RdTools analysis of performance loss rates pre-(blue) and poststorm (orange) for high wind events on all systems even if no outage was detected immediately following the event. The extent of the boxplot represents the interquartile range with the median displayed by a horizontal line within each box. A representative uncertainty bar for each category is indicated by a gray vertical bar.

TABLE III
SUMMARY OF WIND-IMPACTED SYSTEMS

Category (km/h)	Storm	Inverters	Systems	Median PLR (%/year)	Interquartile range (%/year)
<90	pre	5	5	−0.22	0.69
<90	post	5	5	0.16	0.90
90–115	pre	6	6	0.15	1.12
90–115	post	6	6	−1.54	1.68
115–140	pre	56	7	−0.64	0.50
115–140	post	56	7	−1.17	0.92
>140	pre	49	4	−1.15	0.73
>140	post	49	4	−2.18	0.76

analysis alone. One difference with wind-exposed systems is that there are a few inverters at some sites that displayed no increased PLR when most inverters did show higher PLRs at that site. Possible wind shadowing effects could be an explanation; parts of a system could have been sheltered by obstructions in the direction of the approaching storm. Similarly, more information on the individual distributions in each category is provided in Table III.

This wind shadowing phenomenon and the potential importance of the mounting configuration can be seen in an example system of Figs. 8 and 9. The site is located in the desert of the American Southwest and consists of several separate systems using the same modules but different mounting configurations. The difference in PLRs before the high-wind event can be attributed to the systems on building A and the gymnasium being close-mounted to a metal roof leading to an increased module operating temperature, as some of the authors reported

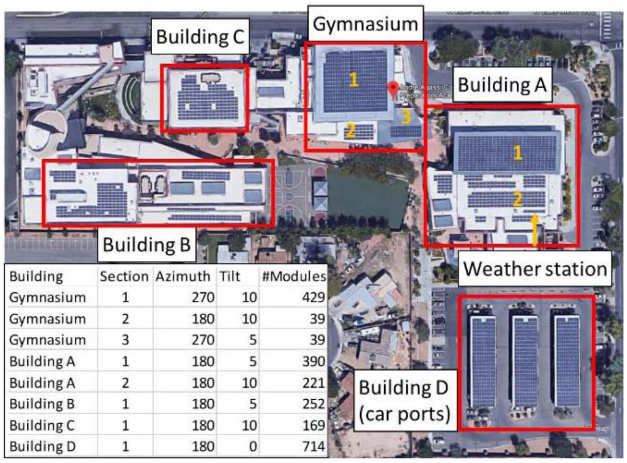

Building	Section	Azimuth	Tilt	#Modules
Gymnasium	1	270	10	429
Gymnasium	2	180	10	39
Gymnasium	3	270	5	39
Building A	1	180	5	390
Building A	2	180	10	221
Building B	1	180	5	252
Building C	1	180	10	169
Building D	1	180	0	714

Fig. 8. Example site consisting of different mounting configurations but the same modules.

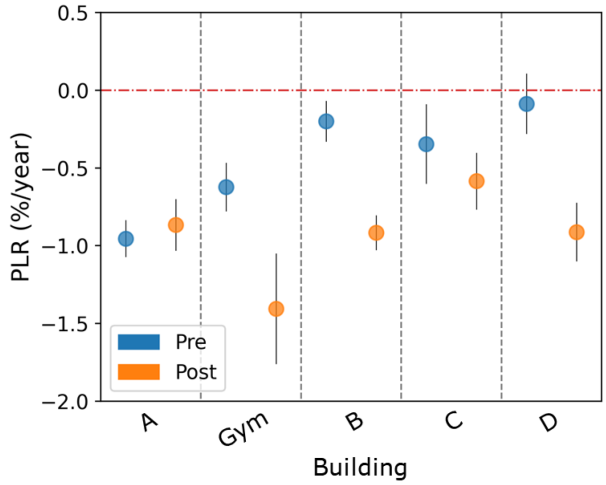

Fig. 9. RdTools analysis of performance loss rates pre-(blue) and poststorm (orange) for one system impacted by a severe wind event in 2014. The systems on all buildings consist of the same modules but different mounting configurations. The extent of the boxplot represents the interquartile range with the median displayed by a horizontal line within each box. A representative uncertainty bar for each category is indicated by a gray vertical bar.

before [14]. The site was exposed to a severe windstorm that was centered to the Northwest of the site and made local headline news. Buildings B and D (the car port) were most exposed and show substantially higher PLRs. The array on building C is surrounded by a high wall and may have provided shelter indicating that mounting configuration may play an important role. The gymnasium (gym) is the highest building at this site and was therefore one of the most exposed. Building A may see some shelter from the taller gymnasium, while the carport system was most exposed exhibiting one of the greatest PLR increases.

A third weather impact analyzed here was large snow loads, which can also lead to damage in PV systems. In Fig. 10, we examined four systems exposed to substantial snowstorms with depth exceeding 0.6 m—25 inches—of snow. The data are colored by snow depth and pressure in Pascals. The weight of snow can vary considerably from 0.2 kg/cm of depth per square meter (m^2) of area of dry snow to ca. 9 kg/(cm m^2) of ice [15].

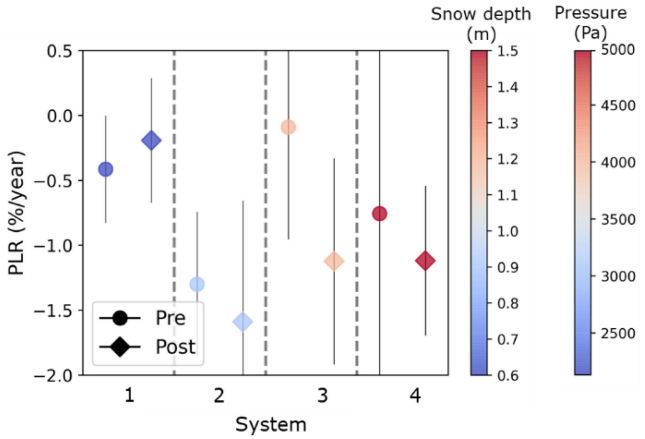

Fig. 10. RdTools analysis of performance loss rates pre and poststorm for four systems exposed to substantial snow events. The color bars indicate the snow depth in meters and resulting pressure in Pascals.

In this case, we used a medium value of typical wet snow of 3.8 kg/(cm m^2). All of these systems were located in northern latitudes making it unlikely that the snow melted quickly after the storms. Additionally, the separate storms that impacted these systems were all associated with considerable wind exposure in late winter. No direct measurements of the water content of the snow exist and will also depend on the temperature during the storm, therefore the conversion into pressure should be considered only as approximate values.

As discussed for hail and wind analysis, the lowest category exhibits marginally less loss after the snow event, which is most likely caused by measurement uncertainty or data quality issues. The three systems that received more than 1 m of snow display slightly increased PLR after the storm, although the uncertainty bars are large because of data quality issues. A paired *t*-test comparing pre to poststorm PLRs of these systems produces a *p*-value of 0.14. *p*-values between 0.05 and 0.2 often are considered not significant. Although *p*-values in this range can indicate a possible correlation, as R. Fisher elaborated in the early 20th century, but more data are needed. The color bar for the load indicates that the highest loads were below the module qualification testing standard of 5400 Pa for mechanical load. However, with additional water content that could easily raise the load by 0.5 kg/(cm m^2), the load would exceed the mechanical load testing in IEC 61215.

V. Conclusion

50-year-old modules and systems are expressed as goals in many research agendas, and a long lifespan is a win for all stakeholders. However, an increased lifespan also increases the probability to exposure of extreme weather. In this article, we have compared two large-scale databases for PV time series and extreme weather to get initial, quantifiable insights into the effects of extreme weather events of PV systems. We determined that median short-term outages lead to production losses of only approximately 1% of annual production per event. Yet, a long tail extending to 60% annual losses is an ominous sign of the risk extreme weather can pose to PV production.

In addition, long-term consequences expressed in higher PLRs that may go undetected can lead to increased financial losses. For hail, we found hail size of 25 mm or above lead to increased performance losses providing a reason for more stringent hail testing currently already under development. System modules qualified through IEC 61215 for 25 mm hail showed higher PLRs when exposed to that same size hail in natural settings. Similarly, a minimum threshold of 90 km/h was found above which higher PLRs can be expected. Although wind shadowing effects from adjacent structures, for example, may mitigate wind impact mounting configuration and installation best practices can decrease performance loss probability [16], [17], [18]. Excessive snow, greater than 1 m, may also lead to increased PLRs although more data are required to definitely establish this connection.

More stringent testing but also more robust modules, and installation practices may be required for more resilient PV systems. However, recent industry trends, such as larger module formats, thinner cells, and thinner front glass, may increase system vulnerability. More data and studies in more geographical locations are needed.

ACKNOWLEDGMENT

The authors would like to thank their corporate partners who provided the PV system data used to perform the analyses in this document. They would also like to thank the NREL PV reliability group, and Katherine Jordan. The views expressed in the article do not necessarily represent the views of the DOE or the U.S. Government. The U.S. Government retains and the publisher, by accepting the article for publication, acknowledges that the U.S. Government retains a nonexclusive, paid-up, irrevocable, worldwide license to publish or reproduce the published form of this work, or allow others to do so, for U.S. Government purposes.

REFERENCES

[1] NOAA National Centers for Environmental Information (NCEI) U.S. Billion-Dollar Weather and Climate Disasters, 2023, doi: 10.25921/stkw-7w73.

[2] H.-O. Pörtner et al., Eds. "IPCC, 2022: Climate change 2022: Impacts, adaptation and vulnerability," in *Contribution of Working Group II to the Sixth Assessment Report of the Intergovernmental Panel on Climate Change*. Cambridge, UK and New York, NY, USA: Cambridge Univ. Press, doi: 10.1017/9781009325844.

[3] C. Deline et al., "Performance index assessment for the PV fleet performance data initiative," in *Proc. IEEE 48th Photovolt. Specialists Conf.*, 2021, pp. 1486–1491, doi: 10.1109/PVSC43889.2021.9518760.

[4] D. C. Jordan et al., "Photovoltaic fleet degradation insights," *Prog. Photovolt.*, vol. 30, no. 10, pp. 1166–1175, 2022.

[5] [Online]. Available: https://www.ncdc.noaa.gov/stormevents/

[6] C. Buerhop et al., "Evolution of cell cracks in PV-modules under field and laboratory conditions," *Prog. Photovolt.*, vol. 26, pp. 261–272, 2018.

[7] T. J. Silverman, N. Bosco, M. Owen-Bellini, C. Libby, and M. G. Deceglie, "Millions of small pressure cycles drive damage in cracked solar cells," *IEEE J. Photovolt.*, vol. 12, no. 4, pp. 1090–1093, Jul. 2022.

[8] M. Deceglie et al., "RdTools v2.1.0 beta.1. Computer software," 2020. [Online]. Available: https://github.com/NREL/rdtools, doi: 10.5281/zenodo.4307010.

[9] M. Sengupta et al., "The national solar radiation data base (NSRDB)," *Renewable Sustain. Energy Rev.*, vol. 89, pp. 51–60, 2018.

[10] D. C. Jordan and C. Hansen, "Clear-sky detection for PV degradation analysis using multiple regression," *Renewable Energy*, vol. 209, pp. 393–400, 2023.

[11] "Terrestrial Photovoltaic (PV) Modules—Design Qualification and Type Approval—Part 1: Test Requirements," IEC 61215-1:2021, 2021.

[12] P. Bostock, "Hail cat: Presenting a method to identify, quantify, and mitigate hail risk," in *Proc. PV Rel. Workshop*, 2023.

[13] "Photovoltaic (PV) Modules—Qualifying Guidelines for Increased Hail Resistance, IEC TS 63397:2022, 2022.

[14] D. C. Jordan, C. Deline, M. Deceglie, T. J. Silverman, and W. Luo, "PV degradation—Mounting & temperature," in *Proc. IEEE 46th Photovolt. Specialists Conf.*, 2019, pp. 0673–0679.

[15] 2022. [Online]. Available: https://roofonline.com/weights-measures/weight-of-snow/?utm_content=expand_article

[16] National Renewable Energy Laboratory, Sandia National Laboratory, SunSpec Alliance, and the SunShot National Laboratory Multiyear Partnership, "Best Practices for Operation and Maintenance of Photovoltaic and Energy Storage Systems", National Renewable Energy Laboratory. Tech. Rep. NREL/TP-7A40-73822, 2018.

[17] C. Burgess, S. Detweiler, C. Needham, and F. Oudheusden, "Solar under storm part II: Select best practices for resilient roof-mount PV systems with hurricane exposure," Clinton Foundation, FCX Solar & Rocky Mountain Institute, 2020.

[18] E. Hotchkiss et al., "Preparing solar photovoltaic, systems against storms," NREL, Tech. Rep. NREL/FS-5R00-81968, May 2022.